J Mol Model (2011) 17:9–19
DOI 10.1007/s00894-010-0695-7

ORIGINAL PAPER

Anthranilate derivatives as TACE inhibitors: Docking based CoMFA and CoMSIA analyses

Malkeet Singh Bahia · Shravan Kumar Gunda · Shwetha Reddy Gade · Saikh Mahmood · Ravikumar Muttineni · Om Silakari

Received: 17 August 2009 / Accepted: 20 February 2010 / Published online: 28 March 2010

Abstract Anthranilic acid based derivatives (ANTs) have been identified as a novel class of potent tumor necrosis factor-α converting enzyme (TACE) inhibitors. A computational strategy based on molecular docking studies, followed by CoMFA and CoMSIA analyses has been performed to elucidate the atomic details of the TACE/ANT interactions and also to identify the most important features impacting TACE inhibitory activity of ANTs. The CoMSIA model resulted to be slightly more predictive than CoMFA model, and gave conventional r^2 0.991, r_{cv}^2 0.793, q^2 0.777, SEE 0.050, F-value 655.610, and r_{test}^2 0.871. The 3D-QSAR field contributions and the structural features of the TACE binding site showed a good correlation. These studies will be useful to design new TACE inhibitors with improved potency.

Keywords TACE inhibitors · CoMFA · CoMSIA · Docking · 3D-QSAR · Rheumatoid arthritis

Electronic supplementary material The online version of this article (doi:10.1007/s00894-010-0695-7) contains supplementary material, which is available to authorized users.

M. S. Bahia · O. Silakari (✉)
Department of Pharmaceutical Science and Drug Research,
Punjabi University,
Patiala, Punjab 147002, India
e-mail: omsilakari@rediffmail.com

S. K. Gunda · S. R. Gade · S. Mahmood
Department of Bioinformatics, Osmania University,
Hyderabad, Andhra Pradesh 150007, India

R. Muttineni
GVK biosciences Pvt. Ltd.,
#210 'My Home Tycoon', 6-3-1192 Begumpet,
Hyderabad, Andhra Pradesh 500016, India

Introduction

TACE [1], a membrane bound Zn endopeptidase [2] was found to be the first mammalian sheddase responsible for cleavage of a variety of membrane proteins including pro-inflammatory cytokine tumor necrosis factor-α (TNF-α), pro-transforming growth factor *alpha* (TGF-α), TNF receptors, β-amyloid precursor protein and L-selectin [3–8]. TACE is mainly responsible for proteolysis of Ala76-Val77 peptide bond of membrane bound proTNF-α. This proteolysis leads to shedding of mature and active form of cytokine, *i.e.*, sTNF-α (soluble TNF-α) from the cells as homotrimer of 17 kDa terminal fragment consisting of 157 nonglycosylated amino acids [9, 10].

TNF-α is a multifunctional pro-inflammatory cytokine involved in inflammation, cell survival, apoptosis and immunity acting *via* two receptors TNF-R1 and TNF-R2 [11] but causes severe damage when it gets produced in an excess amount. Elevated level of TNF-α has been reported in a number of chronic diseases [12–15] like rheumatoid arthritis, inflammatory bowel disease, graft *vs*. host disease, adult respiratory distress syndrome, septic shock, HIV infection [16] and insulin resistance [17]. Although pro-inflammatory cytokines are necessary for survival of human species but as they may cause significant inflammatory damage, their secretion needed to be tightly regulated. Of the many possible strategies to regulate TNF-α production, TACE inhibition has long been viewed as one of the most promising small molecule targets [18]. TACE share many active site similarities with other matrix metalloproteinases (MMPs) and a disintegrin and metalloproteinases (ADAMs) [19, 20]. Therefore, earlier developed TACE inhibitors often suffered from lack of selectivity [21] and broad spectrum MMP inhibition of molecules has been reported as the suspected cause of musculoskeletal side effect [22].

In the present study, computational methodology is applied on a series of potent anthranillic acid derivative class of TACE inhibitors [23–25] with the aim to elucidate the most important TACE-ANT interactions and also to identify features really impacting TACE inhibitory activity of ANTs. On the basis of the crystal structure of TACE, docking simulation [26, 27] was also performed on a selected series of molecules. The most probable docking poses were selected for alignment and submitted to 3D-QSAR studies involving comparative molecular field analysis (CoMFA) [28] and comparative molecular similarity indices analysis (CoMSIA) [28]. Though, there are a few crystal structures for TACE available, the crystal structures are not elucidated for the compounds used for the study. Diverse compounds may bind to the receptor with different orientations and also have induced fit scenario. Hence, generated 3D-computational models can also be used to explore useful suggestions for designing of new TACE inhibitors with improved potency.

Material and methods

Data set

A set of 57 ANTs having common scaffold (shown with bold lining, molecule A in Fig. 1) and their inhibitory activities against TACE were collected from literature [23–25]. Biological activities of all compounds were obtained using same assay method [29]. The reported IC_{50} values were converted into pIC_{50} (-log IC_{50}) values. All study compounds were then grouped into training set and test set on the basis of suggestions given by Oprea *et al*., [30]. Training set and test set consisted of 41 and 16 molecules respectively. Training set was used for model generation and test set for model validation.

Molecular modeling

Three dimensional structures of all ANTs were constructed using Cerius^2 programming package version 4.10 [31] and energy minimization was performed on molecules using CFF95 force field. Further geometric optimization of all molecules was done using semiempirical program MOPAC 6.0 and applying the AM1 Hamiltonian [32].

Docking

For docking of ligands into 3D active site of protein and to estimate binding affinities of docked compounds, an advanced molecular docking program Glide, version 2.5 [33] was used. During docking study, initially Glide performs a complete systemic search for conformational, orientational and positional space of docked ligand and eliminates unwanted conformations using scoring followed by energy optimization. Finally, the conformations are further refined *via* a Monte Carlo sampling of pose conformation. For the present study, X-ray crystal structure of TACE with resolution of 1.9 Å was taken from PDB (ID: 2i47) [34]. The performance of docking method was evaluated by re-docking crystal ligand and correlating the binding pose as well as hydrogen bonding interactions of redocked crystal ligand with original crystal ligand.

The reason behind choosing crystal stricture 2i47 for docking is that the compounds under study were similar to the inhibitor present in 2i47 and hence these compounds may have similar orientation of binding like the inhibitor of selected crystal structure. Then, the conformational deviation of 2i47 will be minimal when the compounds under study will bind to the receptor because of similarity of the compounds with co-crystal. As we are using rigid docking method, 2i47 crystal structure will be the more appropriate choice than any other.

Docking based alignment of molecules

After performing the docking analysis, best/appropriate binding conformations were selected for alignment to be used for 3D QSAR. For the alignment, first of all the best conformation (ranked 1st by the software in terms of docking energy) of the most active compound ANT12 was chosen and validated as best on the basis of formation of

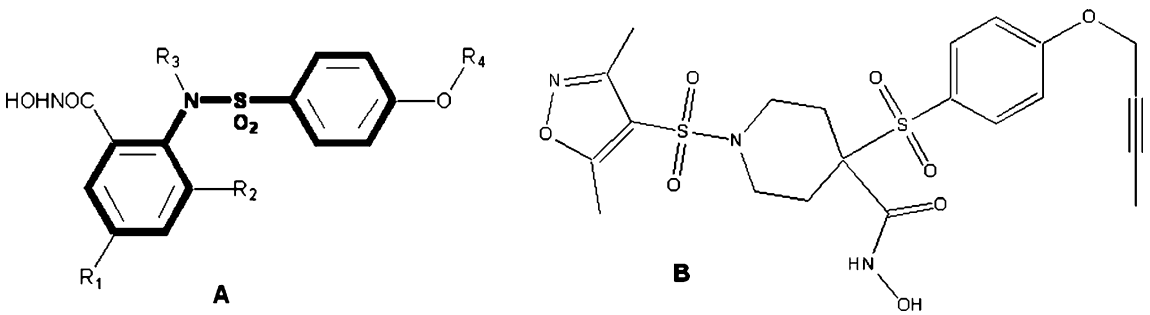

Fig. 1 Common scaffold of ANTs shown in bold lining (**a**); Ligand extracted from PDB 2i47 (**b**)

H-bonds and proper orientation inside the 3D active site (validation was done manually because the best ranked conformation by the software may not be the best always, sometimes it may happen that the best conformation is totally out of the pocket due to steric clashes because it is a constrained docking not the flexible). Then the best conformations of the remaining compounds were selected for the alignment over the best conformation of the most active compound ANT12. During this the best ranked conformations of certain molecules were not aligning then manually the low ranked conformations were checked and appropriate conformations were selected for the alignment (for certain molecules those conformations were aligning which were ranked 13th or 21st by the software, so we named this kind of conformation selection as 'manual selection of appropriate conformations'). This is how the best conformations were evaluated in terms of docking energy and manual observation. Finally selected conformations were aligned and submitted to Sybyl 6.8 [35] for CoMFA and CoMSIA studies.

Field and similarity index calculations

CoMFA method is a widely used 3D-QSAR technique to relate biological activity of a series of molecules with their steric and electrostatic fields. CoMFA potential fields were calculated at each lattice intersection of a regularly spaced grid of 2 Å. The grid box dimensions were determined automatically in such a way that region boundaries were extended 4 Å in each direction from co-ordinates of an aligned bundle of molecules. The van der Waals potential and Columbic terms, which represent steric and electrostatic fields respectively, were calculated using standard Tripos force field method. A sp^3 hybridized carbon atom with +1 charge was used to calculate the CoMFA steric and electrostatic fields respectively. The steric and electrostatic contributions were truncated to +30 kcal mol^{-1} [36].

CoMSIA method calculates five similarity indices: Steric, electrostatic, hydrogen bond donor, hydrogen bond acceptor and hydrophobic parameters. The similarity indices descriptors were calculated using the same lattice box employed for the CoMFA calculations and a sp^3 carbon as probe atom with +1 charge, +1 hydrophobicity, +1 hydrogen bond donor and +1 hydrogen bond acceptor properties [37].

Partial least square analysis and models validation

Partial least square approach [38] is an extension of the multiple regression analysis. It was used to derive the 3D-QSAR models in which CoMFA and CoMSIA descriptors were used as independent variables and pIC_{50} (activity) values as dependent variables. Prior to PLS analysis, column filtering value was set 2.0 kcal mol^{-1} to improve the signal-to-noise ratio.

Leave one out (LOO) cross-validation method was used to check the predictivity of derived model and to identify optimal number of components (ONC). ONC are optimum number of components corresponding to highest q^2 and lowest S_{loo}. The ONC obtained from cross-validation methodology was used in subsequent regression model. To avoid the problem of over prediction and to check the stability and predictability of the generated model different statistical parameters were checked. These statistically parameters are leave one out cross validation (q^2), leave group out cross validation (r_{cv}^2) and boot strapped validation (r_{bs}^2). They are used to determine internal stability and predictability. In leave group out CV different training sets got produced from the original training set (by removal of random groups of molecules) and models are generated by using each of the subset. Then r^2 is calculated for the subsets. In boot strapped validation different training sets got generated by deletion of some molecules from the original training set and some are used more than once and models are generated by using each of the subset. Then if the r_{cv}^2, q^2 and r_{bs}^2 have good values, it indicates that the generated model does not only depend on the original training set because different sub training sets are also used to prove the consistency of correlation. Especially r_{bs}^2 strongly assess the statistical confidence and robustness of derived models and indicate that the model does not depend upon only particular training set.

Final CoMFA and CoMSIA contour models were generated using noncross-validated PLS analysis. To validate the CoMFA and CoMSIA derived models, the predictive ability for the test set of compounds (expressed as r_{pred}^2) was computed with the formula:

$$r^2 = (SD - PRESS)/SD \quad (1)$$

Where SD is the sum of the squared deviations between experimental and mean of experimental biological activities of training set molecules, and PRESS is a sum of squared deviation between predicted and actual activity for every molecule in test set.

Results and discussion

Docking study

For docking study of 57 anthranilate derivatives with TACE, a crystal structure of protein was prepared by removing ligand and solvent coupled with addition of hydrogen atoms. Glide consisted of two modes for docking studies named extra precision (XP) and standard precision

Fig. 2 Superposition of crystal ligand and Glide predicted best docked conformation of inhibitor molecule B; red, crystal ligand; green, docked conformation

(SP). Extra-precision mode is a refinement tool designed for use only on good ligand poses. It is very useful for docking and scoring of the top-ranked poses obtained from standard-precision (SP) mode (Glide documentation). Hence we used SP for docking all the molecules and only high active compounds were docked using XP but there is not much improvement in the posing, so for our experiments we adopted SP mode. The credibility of docking method to predict the bioactive conformation was authenticated using the X-ray structure of TACE in complex with a small molecule ligand inhibitor **B** (Fig. 1). Molecule **B** is a ligand extracted from crystal structure (2i47). The inhibitor **B** was docked into a 3D active site of crystal structure of TACE and docked conformation having lowest docking energy was selected as the most probable bioactive conformation. Glide predicted conformation of inhibitor **B** was perfectly superimposed on X-ray crystallographic structure of the same ligand as shown in Fig. 2. The root mean square deviation (RMSD) between two conformations was found to be 1.263 Å, suggesting high reliability of Glide in terms of reproducing experimentally observed binding mode for TACE inhibitors. Entire 57 ANT molecules were then docked into the active site of protein.

Docking results showed that each of the molecules is forming at least three hydrogen bonds with important amino acids Glu406, Leu348 and Gly349 of protein. Molecules also showed hydrogen bond interactions with other active site amino acids like Pro437 and Val440 of protein. Hydroxamic acid group (-CONHOH) and hydrogen bond acceptor group (-SO_2-) present in all compounds possess hydrogen bonding interactions with important amino acids. Highly active molecules are participating in greater number of interactions with important amino acids Glu406, Leu348 and Gly349 than low active molecules.

The non bonded interactions between highly active molecule ANT12 and amino acids of TACE binding pocket are shown in Fig. 3. As depicted from figure, receptor and ligand are tightly bound to each other by forming a network of hydrogen bonding interactions. The binding between compound and TACE amino acids are depicted as five hydrogen bonding interactions: Two hydrogen bonds between terminal hydroxyl group of hydroxamic acid and 'O' of ionized Glu406 (O.....O, 2.6837 Å and 2.603 Å), a single hydrogen bond between NH of hydroxamic acid group and carbonyl 'O' of Gly349 (O.....N, 2.723 Å), and 'O' of linker sulfonyl group with NH of Leu348 (O.....N, 2.835 Å). A single hydrogen bond is also between terminal hydroxyl and carbonyl 'O' of Val440 (O.....O, 3.034 Å).

Docking based alignment: deriving the bioactive conformations

CoMFA and CoMSIA are mainly based on alignment of molecules having common scaffold. In order to get reliable results molecules were aligned with their corresponding probable bioactive conformations. To derive the appropriate

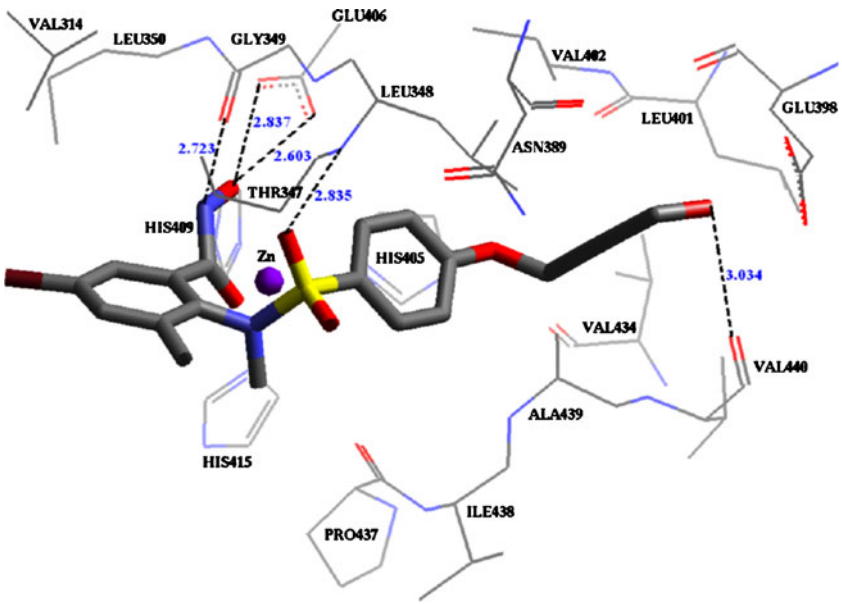

Fig. 3 Docking interactions of molecule ANT12 with active site amino acids of TACE

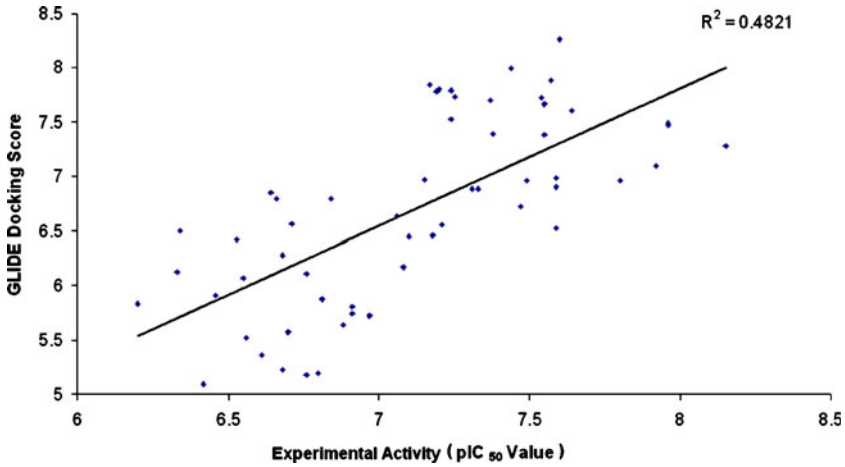

Fig. 4 Correlation graph between biological activity (pIC_{50}) and glide docking score

bioactive conformations, all ANTs were docked with TACE crystal structure using Glide. The correlation plot between biological activity (pIC_{50}) value and glide docking score is shown in Fig. 4 which showed the correlation (r^2) of 0.4821. Finally, best docked conformations of all molecules were selected for alignment on the basis of Glide docking score and manual inspection. Alignment of all ANT molecules is shown in Fig. 5.

CoMFA and CoMSIA studies

From the total set of 57 ANTs, a training set of 41 molecules was used for model generation. An external test set of 16 molecules having structural variation and covering whole ranges of activity was used to validate generated models. CoMFA model was developed using CoMFA steric and electrostatic fields whereas CoMSIA models using steric, electrostatic, hydrophobic, H-bond acceptor and H-bond donor properties as independent variables, and ligand pIC_{50} as dependent variables. The statistical parameters associated with both models are shown in Table 1.

The leave-one-out (LOO) partial least squares (PLS) analysis of generated CoMFA model yielded excellent q^2 value of 0.743, and group out cross validation also yielded good correlation coefficient (r_{cv}^2) of 0.762. Cross validated correlation coefficients are used as a measure of reliability of prediction. Subsequently, conventional statistics were computed using previously obtained ONC value of 5, resulting conventional correlation coefficient (r^2) of 0.983 and F-value of 402.811 with a standard error of estimate (SEE) of 0.070. These conventional statistical measures indicate the goodness of fit of the QSAR model. The predicted pIC_{50} values for each training set compound are given in Table 2 (supporting information). The

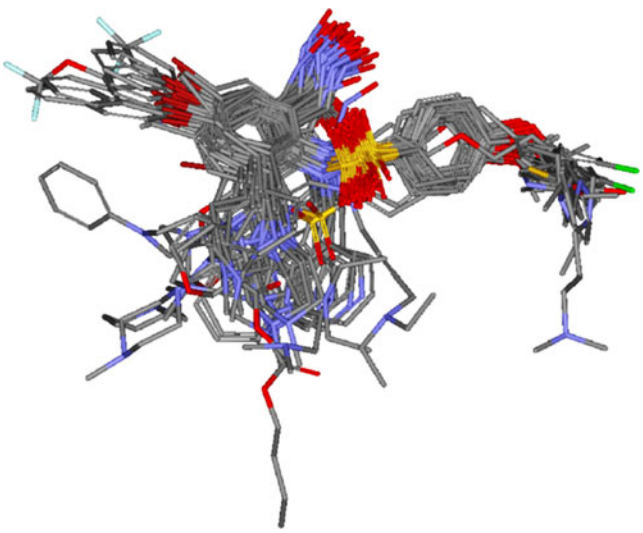

Fig. 5 Superposition of all ANT molecules with common scaffold

Table 1 Summary of CoMFA and CoMSIA studies

Features	CoMFA	CoMSIA
Number of compounds	57	57
Optimum number of components (ONC)	5	6
Leave one out cross validation (q^2)	0.743	0.777
Standard error of prediction (S_{Loo})	0.271	0.256
Group cross validated r^2 (r_{cv}^2)	0.762	0.793
Conventional r^2	0.983	0.991
Standard error of estimate (SEE)	0.070	0.050
F value	402.811	655.610
Steric contribution	0.667	0.180
Electrostatic contribution	0.333	0.303
Hydrophobic contribution	-	0.161
H-bond donor contribution	-	0.168
H-bond acceptor contribution	-	0.189
Bootstrap r^2 (r_{boot}^2)	0.990	0.995
Standard error of estimate (S_{boot})	0.051	0.037
Test set r^2 (r_{pred}^2)	0.862	0.871

relationship between the CoMFA predicted and experimental pIC_{50} values of training set molecules are shown in Fig. 6a.

CoMSIA is an alternative molecular field analysis method to CoMFA. It is tought to be less affected by changes in molecular alignment and provides smoother and interpretable contour maps as a result of employing Gaussian type distance dependence with the molecular similarity indices. CoMSIA was generated using combinations of the following descriptor fields: Steric, electrostatic, hydrophobic, H-bond donor and H-bond acceptor. These descriptors illustrate various properties into spatial locations where they play a decisive role in determining the biological activity. The statistical details of CoMSIA model are summarized in Table 1.

The best model has q^2=0.777, r_{cv}^2=0.793, F-value= 655.610, SEE=0.050 and conventional r^2=0.991 (six ONC). Final predicted pIC_{50} values of training set molecules with CoMSIA model and their residuals are given in Table 2 (supporting information). The experimental activities versus predicted activities in the training set by CoMSIA model are shown in Fig. 6b.

Validation of QSAR models

The validation of QSAR models, which reproduce very well the experimental activity of the training set, was subjected to investigate whether the activity of ANT derivatives can be predicted well with these models. A very important test for the predictability of a QSAR analysis in drug design process is to check ability of model to predict the biological activity of compounds that have not been included in the training set. The predicted verses experimental activity values for the test set are depicted in Fig. 7. Correlation between experimental and predicted activities was calculated for test set compounds (r_{pred}^2) according to the formula suggested by Cramer et al. [36]. The prediction powers of CoMSIA model (r_{pred}^2=0.871) and CoMFA model (r_{pred}^2=0.862) are comparable. Overall, our models exhibited high precision both in regular cross validation and in prediction of activity of test set molecules.

Three dimensional contour map analysis

Contour maps were produced to envision the information content of derived CoMFA and CoMSIA models. The field

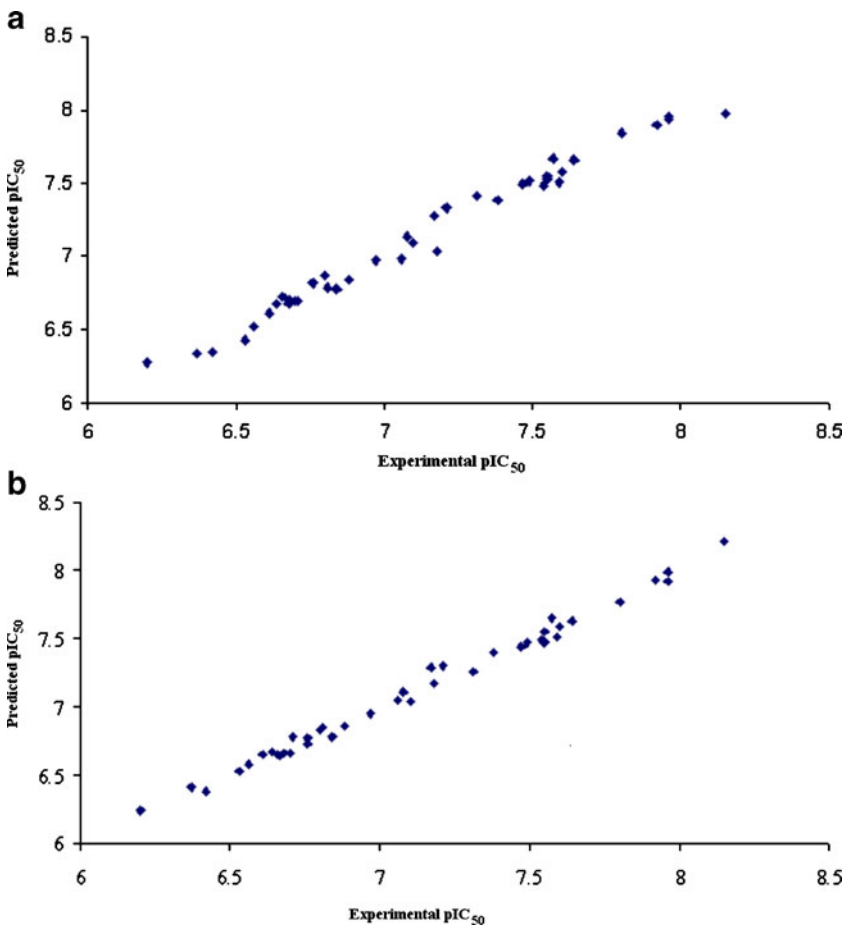

Fig. 6 **a** Distribution of experimental and predicted pIC_{50} values for training set compounds according to CoMFA analysis. **b** Distribution of experimental and predicted pIC_{50} values for training set compounds according to CoMSIA analysis

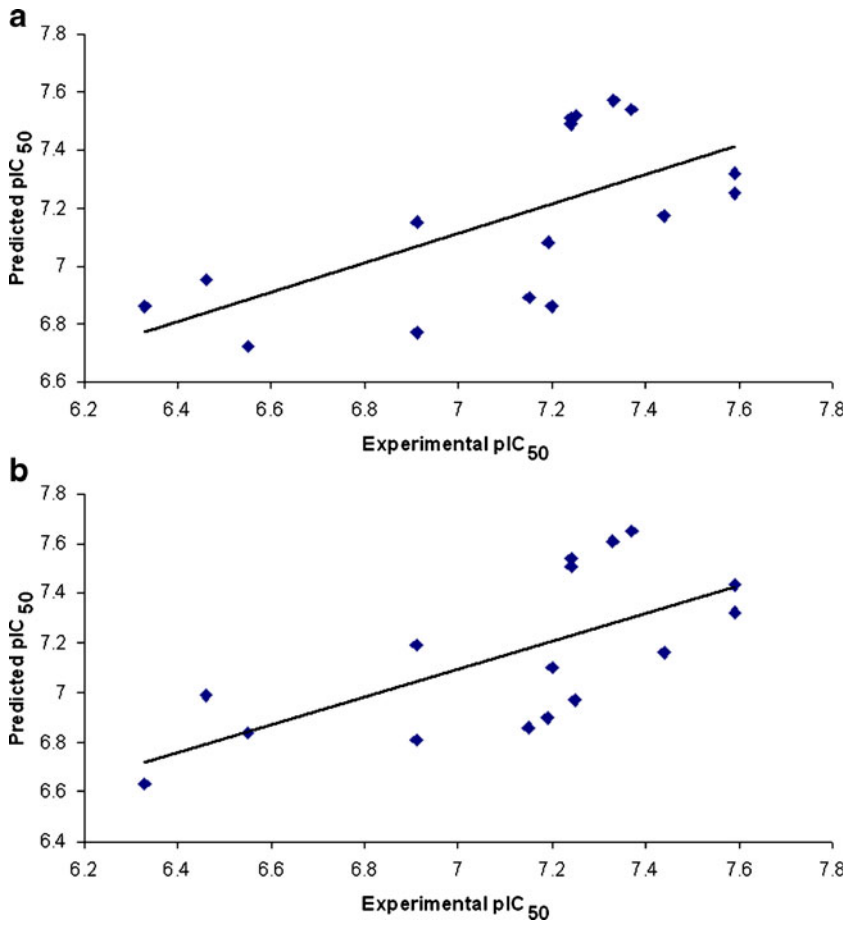

Fig. 7 **a** Distribution of experimental and predicted pIC_{50} values for test set compounds according to CoMFA analysis. **b** Distribution of experimental and predicted pIC_{50} values for test set compounds according to CoMSIA analysis

energies at each lattice point were calculated as the scalar results of the coefficient and the standard deviation associated with a particular column of the data table (stdev * coeff) was plotted as the percentage of the contribution to CoMFA or CoMSIA equation. Stdev * coeff contour plots of CoMFA and CoMSIA for different properties are illustrated in Figs. 8, 9, 10, 11, 12, 13, 14. In these snapshots the most active compound ANT12 is shown in the background as the reference compound. The contour plots help in identifying important regions where any change will subsequently affect the binding preference. Furthermore, they would be helpful in establishing the important features (pharmacophore) contributing to activity and relating them with interactions between the ligand and the active site of receptor.

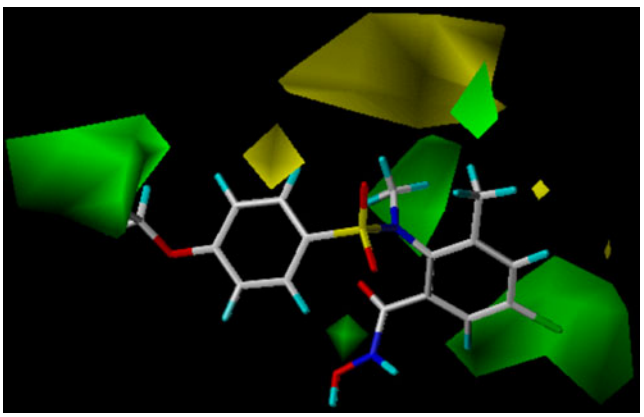

Fig. 8 Contour map of CoMFA steric region for molecule ANT12; green, favored; yellow, disfavored

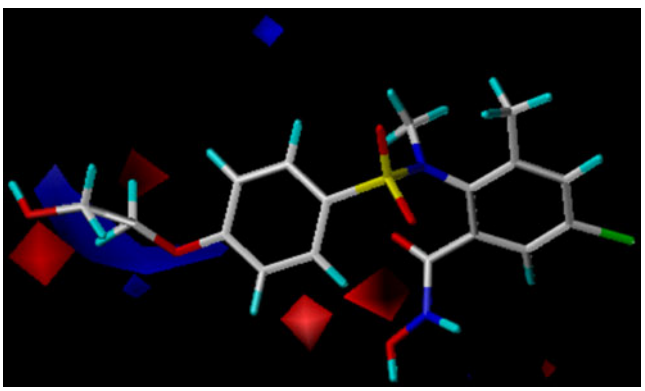

Fig. 9 Contour map of CoMFA electrostatic region for molecule ANT12; blue, favored for electropositive groups; red, disfavored for electronegative groups

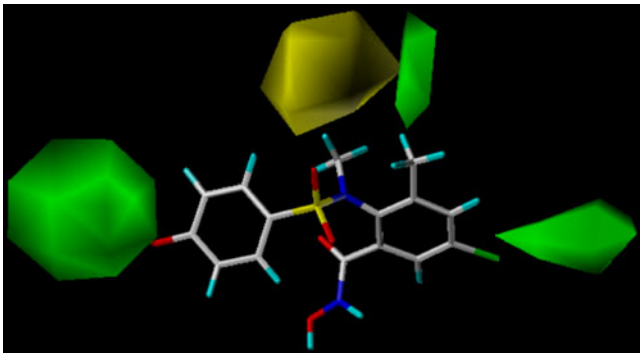

Fig. 10 Contour map of CoMSIA steric region for molecule ANT12; green, favored; yellow, disfavored

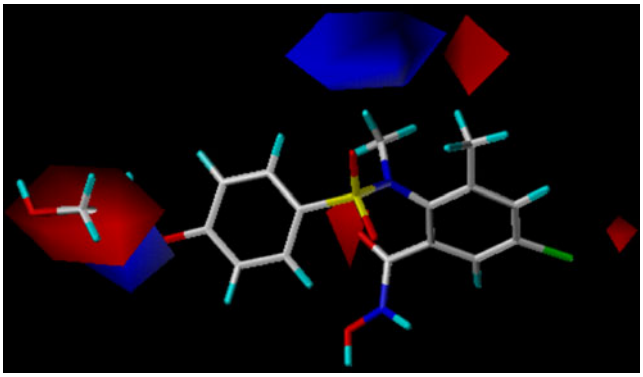

Fig. 12 Contour map of CoMSIA electrostatic region for molecule ANT12; blue, favored for more electropositive groups; red, disfavored for less electropositive and favored for more electronegative groups

CoMFA contours

The steric contours derived from inhibitory data of ANT derivatives using CoMFA is displayed in Fig. 8. The areas indicated by green color correspond to regions, where presence of bulky steric groups is favored and should enhance TACE inhibitory activity of molecule. In contrast, the areas indicated by yellow isopleths correspond to regions where occupancy of steric groups is unfavorable and should be avoided. In Fig. 8 for the highest active molecule ANT12, favorable green isopleths are present close to N-substitution, the 3rd and 5th position of phenyl, and also at the terminal long steric chain attached to benzene sulfonyl ring. On the other hand the unfavorable yellow isopleth is covering over N-substitution and the 3rd position of phenyl ring. Additionally, a small yellow isopleth is also present near 3rd position of phenyl ring. Accordingly, in the highest active molecule its methyl substituent at 'N' atom, a long chain attached to the 4th position of benzene sulfonyl, bromine and methyl substituent at the 5th and 3rd position of phenyl respectively, orient toward favorable green isopleths. Positioning of both yellow and green isopleths over 'N' substitution and the 3rd position of phenyl ring shows that size of substituent at this position is very crucial for inhibitory activity of molecules.

The molecules like ANT**27, 29, 31, 32, 33, 34, 35, 39, 40, 41, 42**. and **43** with bulkier substitutions at linker 'N' atom have lowered activities because bulky substituent at this position are pointed toward sterically unfavorable yellow isopleths and may be causing steric repulsions with active site amino acids. In low active molecules ANT**46, 47, 48, 49, 50, 52, 53, 54, 56**. and **57** bulkier steric group present at the 3rd position of phenyl ring is pointed toward sterically unfavorable yellow isopleth. Green isopleth present close to the 5th position of phenyl ring shows favor of the steric group at this position. In highly active compounds ANT**3, 5, 7, 8, 13, 20**, and **38** sterically favorable bromine group is present at the 5th position of phenyl ring and sterically bulkier chain attached to the 4th position of benzene sulfonyl group is also pointed toward sterically favorable green isopleth.

Electrostatic field contour map of CoMFA analysis is shown in Fig. 9. All compounds correctly positioned their

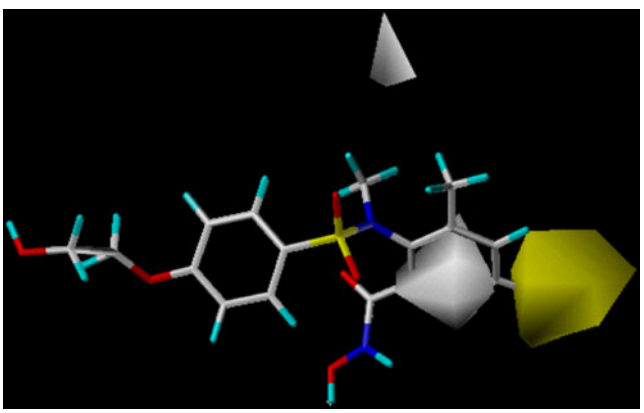

Fig. 11 Contour map of CoMSIA hydrophobic region for molecule ANT12; yellow, favored; white, disfavored

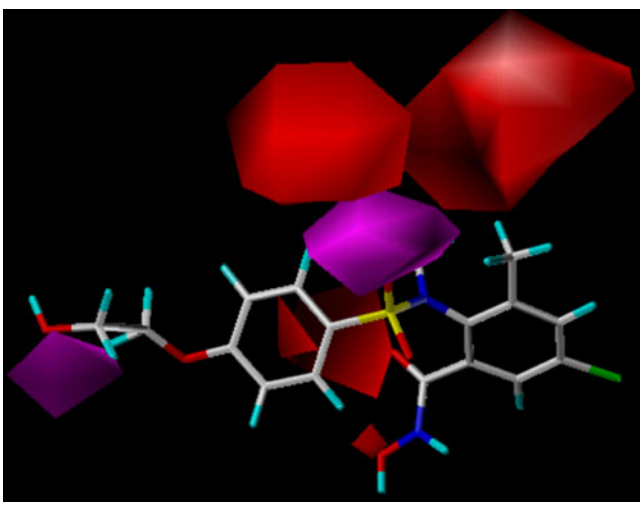

Fig. 13 Contour map of CoMSIA hydrogen bond acceptor region for molecule ANT12; purple, favored; red, disfavored

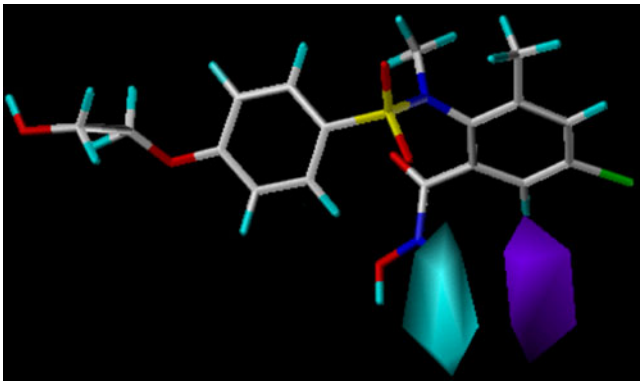

Fig. 14 Contour map of CoMSIA hydrogen bond donor region for molecule ANT12; cyan, favored; purple, disfavored

polar moieties according to distribution of CoMFA electrostatic favorable (blue) and unfavorable (red) regions. Thus, more electropositive substituent are predicted to be favored (blue) around the long stretch of terminal steric chain and at N-substitution whereas more electronegative substituent are predicted to be favored (red) around the C-4 position of steric chain and in the region close to carbonyl 'O' of hydroxamic acid. In Fig. 9, the presence of red isopleths near to carbonyl 'O' of hydroxamic acid and OH at terminus of steric chain (but-2-ynyl) indicates that the electronegative group is favorable at these positions whereas electropositive groups in blue isopleths. In the highest active molecule but-2-ynyl group is attached to etheral 'O', and–$CCCH_2OH$ group is strong electron withdrawing in nature therefore may cause electron deficiency over the carbon attached next to etheral 'O' atom. Due to this positive charge favoring blue region is present at this position.

CoMSIA contours

Steric and hydrophobic

The steric contour plot of CoMSIA is displayed in Fig. 10. Three green and one yellow contour of CoMSIA steric map can be well compared with steric contour maps of CoMFA. It signifies that these isopleths are essentially required for the steric interactions with receptors active site amino acids. Figure 11 shows the hydrophobic contour maps of CoMSIA analysis in which yellow favorable isopleths indicates favorable and white isopleths indicate disfavorable regions for hydrophobic groups in respective regions.

In the most active molecule ANT**12**, a yellow isopleths present near the 5th position of phenyl group favors the presence of the hydrophobic group at this position. In compounds ANT**2, 3, 5, 7, 8, 15, 38**, and **51** the favorable hydrophobic group is also present at the same position. Low activity of molecules ANT**29, 31, 33, 34, 35, 39**, and **40** is due to the presence of hydrophobic groups oriented toward unfavorable white isopleths. A large white isopleths embedded in phenyl ring shows the favorable hydrophilic group at this position and this can be explained on the basis of the resonance of carbonyl group with phenyl ring which make the ring polar and favors the positioning of phenyl and carbonyl group at this position for activity.

Electrostatic contours

The electrostatic contours of CoMSIA in Fig. 12 shows that the pattern of electropositive favorable blue and electronegative favorable red regions can be well compared with that of the electrostatic contour maps of CoMFA shown in Fig. 9. The presence of a similar pattern of electrostatic isopleths in CoMFA and CoMSIA indicates that electrostatic interactions between active site amino acids of TACE and substituents present in these regions is important for the inhibitory activity of ANTs.

H-bond acceptor and donor contours

Figure 13 depicts the contour plots of H-bond acceptor field. Purple isopleths favors the positioning of the hydrogen bond acceptor group in these regions whereas red isopleths disfavored the presence of H-bond acceptor groups. In Fig. 13 purple isopleth is present near the HBA favoring 'O' of sulfonyl group. This group is also proved as a H-bond acceptor in docking studies and formed H-bond with Leu348 acting as H-bond acceptor. One purple isopleths is also present near C-4 position of the steric chain and indicates that the HBA group favors in this region like in molecules ANT**3** and **13**. Two large red isopleths are present over 'N' substitution (molecules ANT**22, 26, 39, 41**, and **42**) and the 3rd position of phenyl group (molecules ANT**30, 47, 49**, and **50**) indicates that the H-bond acceptor group is disfavored in these regions.

The graphical interpretation of the field contributions of H-bond donor is shown in Fig. 14. Cyan contour maps define that position of the H-bond donor group within ligand will be advantageous for binding purposes. For the highly active molecule ANT12 cyan isopleths visible near NH and OH of hydroxamic acid group indicates the favorable H-bonding involving these groups. In the docking study both groups present in the highly active molecule act as H-bond donors and formed hydrogen bond interactions with carbonyl 'O' of Gly349 and ionized 'O' of Glu406.

Comparison of CoMFA, CoMSIA and docking analyses

In order to verify the reliability of 3D QSAR models, CoMFA and CoMSIA models have been compared with

results of docking analysis. Both CoMFA and CoMSIA steric contours proved to match with TACE 3D topology, suggesting steric interactions are important at N-substitution, the 3rd and 5th position of the phenyl ring. The small substituent is favored at the 3rd position of phenyl ring because a small cleft is formed by Thr347, Met345 and Ile438 amino acids, so if the too bulky substituent is present at the same position it may cause the steric clashes with the pocket amino acids. The substituent at the 5th position of phenyl ring is placed within the cleft formed by Val314, Lys315 and Leu350 amino acids so if the bulkier groups are placed at the 5th position they may cause the steric clashes with the said amino acids, so the small substituents are favored at the same position. Optimal sized substituents are also favored at the N-position because too bulky substituents may cause the steric hindrance with the side chains of Pro437, Ile438, Tyr390, Asn389, and Met345 amino acids. Comparison of both analyses also showed that a bulkier chains/group attached to central benzene ring is very important for activity and to occupy the pocket of the enzyme deep inside. This hydrophobic pocket is composed of Val434, Val440, Leu401, Glu398, Val402, Ala439, and Leu348 amino acids and occupancy of this pocket is very important for the inhibition of the TACE. Therefore, the bulky hydrophobic groups at the terminal end of the central benzene ring are favorable for the activity of molecules. Donor and acceptor maps confirm the importance of formation of H-bonds between NH of ligand and carbonyl 'O' of Gyl349, hydroxamic acid OH of ligand and ionized 'O' of Glu406, and also between sulfonyl 'O' of ligand and NH of Leu348 (Fig. 3). Electrostatic property maps are well compared with the docking interactions. The electronegative group present at the terminus of the steric chain is important which is proved by the presence of the H-bond between ligand and Val440 at the same position. Presences of electropositive groups at N-substitution and the 5th position of phenyl ring are also important. Hydrophobic property contour maps are also well compared with docking interactions. The presence of hydrophobic group at the 5th position of phenyl ring is found to be important which is proved by the presence of a chloro group at the same position in the case of molecule ANT12. In the case of other molecules bromo, methyl and phenyl groups are also present which explain the statement.

Concluding remarks

The 3D-QSAR field contributions showed good correlation with 3D topology of TACE. CoMFA and CoMSIA analyses highlighted the important features impacting the inhibitory activity of molecules. On the basis of the present study it can be concluded that:

➢ Both analyses showed the importance of bulky steric chain at the 4th position of benzene sulfonyl group to occupy the pocket of enzyme deep inside.
➢ Small steric substitutions at linker 'N' atom, the 3rd and 5th positions of phenyl ring are shown to be favorable but not the large ones (optimal size).
➢ The CoMSIA hydrophobic map points out the beneficial presence of small hydrophobic substitutes at the 5th position of phenyl ring and unfavorable presence of large hydrophobic groups at the linker 'N' position because the large group at this position may feel steric clashes with active site amino acids.
➢ Contour maps showed the importance of H-bond donor and acceptor groups and the presence of their respective positions also. Contributions of all fields are also well correlated with docking analysis.

In the future information elaborated by these models can be exploited to design new TACE inhibitors with improved potency and to predict their activity prior to synthesis.

References

1. Black RA (2002) Tumor necrosis factor-α converting enzyme. Int J Biochem Cell Biol 34:1–5
2. Duan JJW, Lu Z, Wasserman ZR, Liu RQ, Covington MB, Decicco CP (2005) Non-hydroxamate 5-phenylpyrimidine-2, 4, 6-trione derivatives as selective inhibitors of tumor necrosis factor-α converting enzyme. Bioorg Med Chem Lett 15:2970–2973
3. Marcia LM, Judith MW, Millard HL, Robert CA (2001) TACE and other ADAM proteases as targets for drug discovery. Drug Discov Today 6:417–426
4. Black RA, Rauch CT, Kozlosky CJ, Peschon JJ, Slack JL, Wolfson MF, Castner BJ, Stocking KL, Reddy P, Srinivasan S, Nelson N, Boiani N, Schooley KA, Gerhart M, Davis R, Fitzner JN, Johnson RS, Paxton RJ, March CJ, Cerretti DP (1997) A metalloprotease disintegrin that releases tumor necrosis factor-α from cells. Nature 385:729–733
5. Moss ML, Jin SLC, Milla ME, Burkhart W, Carter HL, Chen WJ, Clay WC, Didsbury JR, Hassler D, Hoffmann CR, Kost TA (1997) Clonning of a disintegrin metalloprotease that processes precusor tumor necrosis faactor-α. Nature 385:733–736
6. Peschon JJ, Slack JL, Reddy P, Stocking KL, Sunnaeburg SW, Lee DC, Russel WE, Castner BJ, Johnson RS, Fitzner JN, Boyce RW, Melson N, Kozlosky CJ, Wolfson MF, Rauch CT, Cerretti DP, Paxton RJ, March CJ, Black RA (1998) An essential role for ectodomain shedding in mammalian development. Science 282:1281–1284
7. Mezyk R, Bzowska M, Bereta J (2003) Structure and functions of tumor necrosis fsctor-α converting enzyme. J Acta Biochim Pol 50:625–645
8. Buxbaum JD, Liu KN, Luo Y, Slack JL, Stocking KL, Peschon JJ, Johnson RS, Castner BJ, Cerretti DP, Black RA (1998) Evidence that tumor necrosis factor-α converting enzyme is involved in regulated α-secratase cleavage of the alzheime amyloid protein precursor. J Biol Chem 273:27765–27767

9. Xue CB, He X, Roderick J, Corbett RL, Duan JJW, Liu RQ, Covington MB, Newton RC, Trzaskos JM, Magolda RL, Wexler RR, Decicco CP (2003) Rational design, synthesis and structure activity relationships of a cyclic succinate series of TNF-α converting enzyme inhbitors. Part 1: lead identification. Bioorg Med Chem Lett 13:4293–4297
10. Letavic MA, Axt MZ, Barberia JT, Carty TJ, Danley DE, Geoghegan KF, Halim NS, Hoth LR, Kamath AV, Laird ER, LoprestiMorrow LL, McClure KF, Mitchell PG, Natarajan V, Noe MC, Pandit J, Reeves L, Schulte GK, Snow SL, Sweeney FJ, Tan DH, Yu CH (2002) Synthesis and biological activity of selective pipecolic acid based TNF-α converting inhibitors. Bioorg Med Chem Lett 12:1387–1390
11. Bazzoni F, Beutler B (1996) The tumor necrosis factor ligand and receptor families. N Engl J Med 334:1717–1725
12. Sekut L, Connolly KM (1996) Pathophysiology and regulation of TNF-α in inflammation. Drug News Perspect 9:261–269
13. Rink L, Kirchner H (1996) Recent progress in the tumor necrosis factor-α field. Int Arch Allergy Immunol 111:199–209
14. Brennan FM, Maini RN, Walport M (1992) TNF-α: a pivotal role in rheumatoid arthritis? Br J Rheumatol 31:293–298
15. Maini RN, Brennan FM, Williams R, Chu CQ, Cope AP, Gibbons D, Elliot M, Feldmann M (1993) TNF-α in rheumatoid arthritis and prospects of anti-TNF therapy. Clin Exp Rheumatol 11:S173–S175
16. Kitano K, Rivas CI, Baldwin GC, Vera JC, Golde DW (1993) Tumor necrosis factor dependent production of human immunodeficiency virus 1 in chronically infected HL-60 cells. Blood 82:2742–2748
17. Hotamisligil GS, Spiegelman BM (1994) Tumor necrosis factor-α: a key component of the obesity diabetes link. Diabetes 43:1271–1278
18. Newton RC, Solomon KA, Covington MB, Decicco CP, Haley PJ, Friedman SM, Vaddi K (2001) Biology of TACE inhibition. Ann Rheum Dis 60:25–32
19. Lukacova V, Zhang Y, Kroll DM, Raha S, Comez D, Balaz SA (2005) A comparison of the binding site of matrix metalloproteinases and tumor necrosis factor-α converting enzyme: implications for selectivity. J Med Chem 48:2361–2370
20. Maskos K, Fernandez-Catalan C, Huber R, Bourenkov G, Bartunik H, Ellestad G, Reddy P, Wolfson M, Rauch C, Castner B, Davis R, Clark H, Petersen M, Fitzner J, Cerratti D, March C, Paxton R, Black R, Bode W (1998) Crystal structure of the catalytic domain of human tumor necrosis factor-α converting enzyme. Proc Natl Acad Sci USA 95:3408–3412
21. Renkiewicz R, Qiu L, Lesch C, Un X, Devalaraja R, Cody T, Kaldjian E, Welgus H, Baragi V (2003) Broad spectrum matrix metalloproteinase inhibitor marimastat induced musculoskeletal side effects in rats. Arthritis Rheum 48:1742–1749
22. Script (1998) 20:2349
23. Levin JI, Chen JM, Du MT, Nelson FC, Killar LM, Skala S, Sung A, Jin G, Cowling R, Barone D, March CJ, Mohler KM, Black RA, Skotnicki JS (2002) Anhranilate sulfonamide hydroxamate TACE inhibitors. Part 2: SAR of the acetylenic P1′ group. Bioorg Med Chem Lett 12:1199–1202
24. Levin JI, Chen J, Du M, Hogan M, Kincaid S, Nelson FC, Venkatesan AM, Wehr T, Zask A, DiJoseph J, Killar LM, Skala S, Sung A, Sharr M, Roth C, Jin G, Cowling R, Mohler KM, Black RA, March CJ, Skotnicki JS (2001) The discovery of anthranilic acidbased MMP inhibitors. Part 2: SAR of the 5-position and P1′ group. Bioorg Med Chem Lett 11:2189–2192
25. Levin JI, Chen JM, Du MT, Nelson FC, Wehr T, Di Joseph JF, Killar LM, Skala S, Sung A, Sharr MA, Roth CE, Jin G, Cowling R, Di L, Sherman M, Xu ZB, March CJ, Mohler KM, Black RA, Skotnicki JS (2001) The discovery of anthranilic acid based MMP inhibitors. Part 3: incorporation of basic amines. Bioorg Med Chem Lett 11:2975–2978
26. Lybrand TP (1995) Ligand-protein docking and rational drug design. Curr Opin Struct Biol 5:224–228
27. Kitchen DB, Furr JR (2004) Docking and scoring in virtual screening for drug discovery: methods and applications. Nat Rev Drug Discov 3:935–949
28. Cichero E, Cesarini S, Fossa P, Spallarossa A, Mosti L (2009) Thiocarbamates as non-nucleoside HIV-1 reverse transcriptase inhibitors: docking based CoMFA and CoMSIA analysis. Eu J Med Chem 44:2059–2070
29. Jin G, Black R, Wolfson M, Rauch C, Ellestad GA, Cowling R (2002) A continuous fluorimetric assay for tumor necrosis factor-α converting enzyme. Anal Biochem 302:269–275
30. Oprea TI, Waller CL, Marshell GR (1994) Three dimensional quantitative structure activity relationship of human immunodeficiency virus (I) protease inhibitors-2: predictive power using limited exploration of alternate binding modes. J Med Chem 37:2206–2215
31. Cerius2 software, Version 4.10. Accelrys, Burlington, MA
32. Dewar MJS, Zoebish EG, Healy EF, Stewart JP (1985) Development and use of quantum molecular models.76. AM1: a new general purpose quantum mechanical molecular model. J Am Chem Soc 107:3902–3909
33. Glide.http://www.schrodinger.com
34. Condon JS, McCarthy DJ, Levin JI, Lombart HG, Lovering FE, Sun L, Wang W, Xua W, Zhang Y (2007) Identification of potent and selective TACE inhibitors via the S1 pocket. Bioorg Med Chem Lett 17:34–39
35. SYBYL, Version 6.8 (2000) Tripos Associates, St. Louis, MO
36. Cramer RD III, Patterson DE, Bunce JD (1988) Comperative molecular field analysis (CoMFA): effect of shape on binding of steroids to carrier proteins. J Am Chem Soc 110:5959–5967
37. Klebe G, Abraham U, Mietzner T (1994) Molecular similarity indices in Comparative analysis (CoMSIA) of drug molecules to correlate and predict their biological activity. J Med Chem 37:4130–4146
38. Wold S, Lindgerg W, Persson JA (1983) Partial least squares method for spectrofluorimetric analysis of mixtures of humic acid and lignin sulfonate. Anal Chem 55:643–648